Fiber-optic waveguide coupled surface plasmon resonance sensor

Jae Heon Ahn,[1,2] Tae Yeon Seong,[2] Won Mok Kim,[1] Taek Sung Lee,[1] Inho Kim, [1] and Kyeong-Seok Lee[1,*]

[1]*Electronic Materials Research Center, Korea Institute of Science and Technology, Seoul 136-791, South Korea*
[2]*Department of Materials Science and Engineering, Korea University, Seoul 136-713, South Korea*
[*]*kslee21@kist.re.kr*

Abstract: A novel approach to give an excellent tunability and self-referencing capability was presented by applying a concept of waveguide coupled surface plasmon resonance mode to a fiber-optic sensor. The presence of dielectric waveguide sandwiched between two metal layers made it possible to precisely tune the resonance wavelength in a broad range from visible to infrared region and to generate multiple modes which may be selectively used for suitable applications. Our approach also verified the potential capability of self-referencing based on a remarkable difference in sensitivity between the plasmonic and waveguide modes excited by p- and s-polarized lights, respectively, without using an additional reference channel. Experimental measurement carried out on sucrose solutions with varying concentration demonstrated the feasibility of our approach.

OCIS codes: (130.6010) Sensors; (240.6680) Surface plasmons; (060.2370) Fiber optic sensors; (280.4788) Optical sensing and sensors.

References and links

1. R. C. Jorgenson and S. S. Yee, "A fiber-optic chemical sensor based on surface plasmon resonance," Sens. Actuators B Chem. **12**(3), 213–220 (1993).
2. A. K. Sharma, R. Jha, and B. D. Gupta, "Fiber-optic sensors based on surface plasmon resonance: A comprehensive review," IEEE Sens. J. **7**(8), 1118–1129 (2007).
3. C. Perrotton, N. Javahiraly, M. Slaman, B. Dam, and P. Meyrueis, "Fiber optic surface plasmon resonance sensor based on wavelength modulation for hydrogen sensing," Opt. Express **19**(S6 Suppl 6), A1175–A1183 (2011).
4. D. Monzón-Hernández, J. Villatoro, D. Talavera, and D. Luna-Moreno, "Optical-fiber surface-plasmon resonance sensor with multiple resonance peaks," Appl. Opt. **43**(6), 1216–1220 (2004).
5. R. Kashyap and G. Nemova, "Surface plasmon resonance-based fiber and planar waveguide sensors," J. Sens. **2009**, 1–9 (2009).
6. B. D. Gupta and R. K. Verma, "Surface plasmon resonance-based fiber optic sensors: principle, probe designs, and some applications," J. Sens. 1–12 (2009).
7. S. M. Tripathi, A. Kumar, E. Marin, and J. P. Meunier, "Side-polished optical fiber grating-based refractive index sensors utilizing the pure surface plasmon polariton," J. Lightwave Technol. **26**(13), 1980–1985 (2008).
8. Z. Y. Zhang, P. Zhao, F. G. Sun, G. Z. Xiao, and Y. M. Wu, "Self-referencing in optical-fiber surface plasmon resonance sensors," IEEE Photon. Technol. Lett. **19**(24), 1958–1960 (2007).
9. W. Peng, S. Banerji, Y. C. Kim, and K. S. Booksh, "Investigation of dual-channel fiber-optic surface plasmon resonance sensing for biological applications," Opt. Lett. **30**(22), 2988–2990 (2005).
10. E. K. Akowuah, T. Gorman, S. Haxha, and J. V. Oliver, "Dual channel planar waveguide surface plasmon resonance biosensor for an aqueous environment," Opt. Express **18**(24), 24412–24422 (2010).
11. L. L. Obando and K. S. Booksh, "Tuning dynamic range and sensitivity of white-light, multimode, fiber-optic surface plasmon resonance sensors," Anal. Chem. **71**(22), 5116–5122 (1999).
12. R. Slavik, J. Homola, and J. Ctyroky, "Miniaturization of fiber optic surface plasmon resonance sensor," Sens. Actuators B Chem. **51**(1-3), 311–315 (1998).
13. A. Lahav, A. Shalabaney, and I. Abdulhalim, "Surface plasmon sensor with enhanced sensitivity using top nano dielectric layer," J Nanophotonics **3**, 031501 (2009).
14. A. Shalabney and I. Abdulhalim, "Figure-of-merit enhancement of surface plasmon resonance sensors in the spectral interrogation," Opt. Lett. **37**(7), 1175–1177 (2012).
15. J. T. Hastings, J. Guo, P. D. Keathley, P. B. Kumaresh, Y. Wei, S. Law, and L. G. Bachas, "Optimal self-referenced sensing using long- and short- range surface plasmons," Opt. Express **15**(26), 17661–17672 (2007).
16. F. C. Chien and S. J. Chen, "A sensitivity comparison of optical biosensors based on four different surface plasmon resonance modes," Biosens. Bioelectron. **20**(3), 633–642 (2004).

#172755 - $15.00 USD Received 17 Jul 2012; revised 4 Sep 2012; accepted 4 Sep 2012; published 6 Sep 2012

17. K. S. Lee, J. M. Son, D. Y. Jeong, T. S. Lee, and W. M. Kim, "Resolution enhancement in surface plasmon resonance sensor based on waveguide coupled mode by combining a bimetallic approach," Sensors (Basel) **10**(12), 11390–11399 (2010).
18. H. Y. Lin, Y. C. Tsao, W. H. Tsai, Y. W. Yang, T. R. Yan, and B. C. Sheu, "Development and application of side-polished fiber immunosensor based on surface plasmon resonance for the detection of Legionella pneumophila with halogens light and 850 nm-LED," Sens. Actuators A Phys. **138**(2), 299–305 (2007).
19. H. Y. Lin, W. H. Tsai, Y. C. Tsao, and B. C. Sheu, "Side-polished multimode fiber biosensor based on surface plasmon resonance with halogen light," Appl. Opt. **46**(5), 800–806 (2007).
20. J. Homola, "Surface plasmon resonance sensors for detection of chemical and biological species," Chem. Rev. **108**(2), 462–493 (2008).
21. T. Okamoto and I. Yamaguchi, "Absorption measurement using a leaky waveguide mode," Opt. Rev. **4**(3), 354–357 (1997).
22. Film Wizard™, Optical Thin Film software, (Scientific Computing International, Carlsbad, CA, USA). http://www.sci-soft.com/Film%20Wizard.htm.
23. Y. Xu, N. B. Jones, J. C. Fothergill, and C. D. Hanning, "Analytical estimates of the characteristics of surface plasmon resonance fibre-optic sensors," J. Mod. Opt. **47**(6), 1099–1110 (2000).
24. Ocean Optics Product Catalog, (2012). http://www.oceanoptics.com/catalog/Ocean_Optics_Catalog_2012.pdf.
25. I. Garcés, C. Aldea, and J. Mateo, "Four-layer chemical fibre optic plasmon-based sensor," Sens. Actuators B Chem. **7**(1-3), 771–774 (1992).
26. C. Caucheteur, C. Chen, V. Voisin, P. Berini, and J. Albert, "A thin metal sheath lifts the EH to HE degeneracy in the cladding mode refractometric sensitivity of optical fiber sensors," Appl. Phys. Lett. **99**(4), 041118 (2011).
27. B. P. Nelson, A. G. Frutos, J. M. Brockman, and R. M. Corn, "Near-infrared surface plasmon resonance measurements of ultrathin films. 1. angle shift and SPR imaging experiments," Anal. Chem. **71**(18), 3928–3934 (1999).
28. R. Ziblat, V. Lirtsman, D. Davidov, and B. Aroeti, "Infrared surface plasmon resonance: A novel tool for real time sensing of variations in living cells," Biophys. J. **90**(7), 2592–2599 (2006).
29. S. Herminjard, L. Sirigu, H. P. Herzig, E. Studemann, A. Crottini, J. P. Pellaux, T. Gresch, M. Fischer, and J. Faist, "Surface plasmon resonance sensor showing enhanced sensitivity for CO2 detection in the mid-infrared range," Opt. Express **17**(1), 293–303 (2009).

1. Introduction

Since Jorgenson and Yee have proposed optical fiber for surface plasmon resonance (SPR) sensing at 1993, fiber-optic SPR sensors have received considerable attention due to their simple measurement system, low cost fabrication, and capability of remote sensing [1–3]. They are especially useful for in situ detection on protein concentrations in biological fluids, air and water quality, and remote sensing for process control in industries. These sensors also take advantages of high sensitivity and label free detection of conventional prism-coupled SPR sensor. Various configurations have been proposed and implemented to provide a desirable performance of fiber-optic SPR sensors [4–7]. In spite of some notable achievements, there still exist several challenging issues regarding the tunability of operation range and a reference-compensated calibration of SPR signal from system instabilities such as temperature change, fiber bending, and light source fluctuation, which has recently attracted increasing concerns [4, 8–11].

Regardless of type of fibers, single or multimode, being used in conventional fiber-optic SPR sensor, the degree of freedom in controlling the resonance wavelength is highly restricted, which we will discuss in more detail in the following section. One simple way of tuning the SPR wavelength is to add a thin dielectric-overlayer coating on Au surface [12]. However, it sacrifices the merit of using Au surface by disabling the well-established Au surface chemistry for biospecific binding. Besides, the location of analytes apart from the Au surface where the evanescent field has maximum may reduce the sensitivity of sensor. On the other hand, it should be noted that the effect of dielectric overlayer remains open to dispute as recent works reported that the nano dielectric overlayer with high refractive index rather enhances the sensitivity of the sensor and even improve the local field near the surface [13, 14]. As effective alternatives, approaches to modify the incident angle condition by tapering the distal-end of multimode fiber [11] or to generate multiple hybrid surface plasmon modes by forming an asymmetric thin metallic shell on a tapered zone of single mode fiber have been suggested [4].

Another important issue lies in a reference-compensated calibration of SPR signal. The most widely adopted way is to form an additional reference channel beside a signal channel on the same fiber [8–10]. The surface of cascade-type reference channel is usually blocked by

#172755 - $15.00 USD Received 17 Jul 2012; revised 4 Sep 2012; accepted 4 Sep 2012; published 6 Sep 2012

a thick dielectric film so that the evanescent field doesn't reach target analytes or covered with a receptor only responding to non-specific effects. Recently, another self-referencing scheme has been reported in a Kretchman-Raether prism coupler configuration, which takes advantage of the difference in sensitivity of both the long- and short-range SPR modes [15]. This scheme is advantageous over the cascade-type method in that the modes are excited simultaneously at the exactly same sensing surface. However, the symmetric index requirement to excite the coupled modes restricts its application.

In this study, we present and demonstrate a new route to give an excellent tunability in operation wavelength of fiber-optic SPR sensor and a novel scheme of self-referencing. For this purpose, we adopted a concept of waveguide coupled SPR mode [16, 17] to the fiber-optic sensor for the first time. Theoretical modeling was carried out to explore the characteristics of fiber-optic waveguide coupled SPR (WCSPR) sensor. As a model structure, multilayer stacks consisting of inner-metal layer\dielectric waveguide\outer-metal layer were applied to the side-polished multimode fiber (MMF) with a SiO_2 core and compared with the conventional case of using a Au single layer. The effects of presence of dielectric waveguide on the SPR properties and the sensor performance were investigated theoretically and experimentally.

2. Sensor configuration and experiments

A schematic configuration of side-polished fiber-optic WCSPR sensor presented here is illustrated in Fig. 1(a). The WCSPR stack consists of a dielectric waveguide sandwiched between two adjacent metal layers. The side-polished planar region of MMF is beneficial for deposition of multilayer stack [18, 19]. Two major distinctive distributions of electric field (E-field) expected to be peculiar to our approach are indicated in the Fig. 1(a). One is the E-field confined near the outer-Au surface and exponentially decays away from it. It results from the plasmonic mode coupled though the waveguide and excited by a p-polarized light [20]. For the coupling to take place, another surface plasmon mode oscillating in the waveguide region (although it's not shown in Fig. 1(a)) should be present with its field maximum at Au-

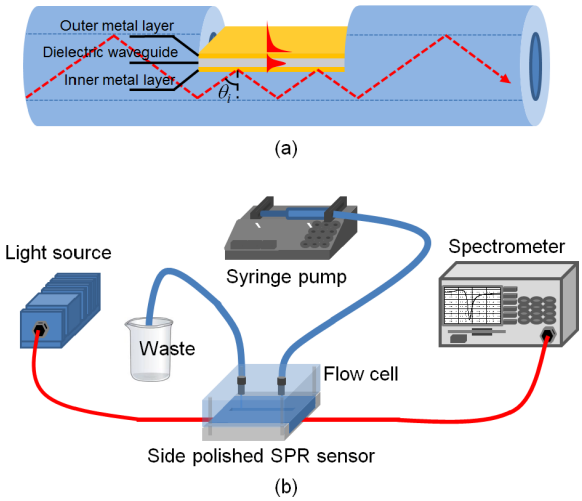

Fig. 1. (a) Schematic configuration of side-polished fiber-optic WCSPR sensor and (b) experimental setup for measuring the sensing performance.

waveguide boundary. The other one is due to a waveguide mode generated by a s-polarized light, in which most energy is confined within the waveguide and only weak leaky fields exist outside it [21]. Such a distinction in E-field distribution would play a major role in determining the sensor characteristics.

#172755 - $15.00 USD Received 17 Jul 2012; revised 4 Sep 2012; accepted 4 Sep 2012; published 6 Sep 2012

For the theoretical analysis, a multilayer optics for the model structure consisting of SiO_2 incident medium\inner-Au layer\ZnS-SiO_2 waveguide\outer-Au layer was calculated using commercial optical thin film software (SCI Film WizardTM) [22]. The internal reflectance inside the SiO_2 fiber core was systematically investigated in a water buffer (n_s = 1.332) as a function of various parameters such as incident angle, light wavelength and polarization, thicknesses of dielectric waveguide and inner- and/or outer-Au layers, and the refractive index change in surrounding medium.

Based on the theoretical calculation, fiber-optic WCSPR sensor was fabricated. Step-index MMFs with a SiO_2 core of 200 μm diameter were used and side-polished down to about half of core diameter using a diamond polishing film. The side-polished length was 20 mm and the planar surface was then coated with a model stack of inner-Au (18 nm)\ZnS-SiO_2 waveguide (220 nm)\outer-Au (18 nm) by RF magnetron sputtering method at room temperature. The working pressure was 0.67 Pa (5 mTorr) in pure Ar atmosphere. The RF power was set to 80 W for ceramic ZnS-SiO_2 target and 20 W for metallic Au. All targets are 2 in. in diameter. To improve the adhesion between the SiO_2 core and inner-Au layer, 2 nm thickness of Ti layer was inserted between them. The thickness of each layer was adjusted from the deposition rate experimentally determined under the same condition.

The SPR characteristics of fabricated fiber-optic sensor and the response to an environmental change were analyzed using an experimental setup shown in Fig. 1(b). A white light from a tungsten-halogen lamp (LS-1, ocean optics) was used as a light source and directly coupled to the fiber through the SMA 905 connector. The transmitted spectra were then measured by a spectrometer (HR2000CG + UV-NIR, ocean optics) connected to the other end of fiber and normalized with respect to the light source spectrum acquired from the same side-polished fiber before the deposition of plasmonic multilayer stack. A home-made flow-cell was attached to the sensing surface and sucrose solutions of different concentration were delivered to the flow cell using a syringe pump (PHD2000, Harvard Apparatus) for the analysis of sensor performance.

3. Results and discussion

Figure 2 shows two-dimensional (2D) contour maps of internal reflectance calculated inside the silica core for both s- and p-polarization as a function of wavelength and incident angle θ_i for the multilayer stacks of conventional SPR and WCSPR fiber-optic sensors. Here, the s- and p-polarization was defined with respect to the plane of incidence that the incident light makes when reflected from the planar region of multilayer stack. The red region indicates a total reflection and the dark blue streak regions represent reflectance dips arising from the excitation of waveguide or plasmonic modes. For the conventional fiber-optic SPR sensor, we assumed a single Au layer of 45-nm thickness. It is obvious that only one SPR mode is generated by p-wave polarization [Fig. 2(a)] and there is no guided mode by s-wave [Fig. 2(c)]. On the other hand, both the SPR modes by p-wave [Fig. 2(b)] and the waveguide modes by s-wave [Fig. 2(d)] are observed in the WCSPR stack. It is also noted here that it has multiple resonance dips in contrast to the conventional sensor. The multilayer stack used in this calculation is SiO_2 core\inner-Au layer (18 nm)\ZnS-SiO_2 waveguide (400 nm)\outer-Au layer (18 nm)\water buffer.

Examining the Fig. 2(a) revealed the problem inherent to the conventional fiber-optic SPR sensor. Since the fiber-optic SPR sensor includes no mechanical moving parts for satisfying the phase matching condition, the internal incident angle θ_i in the core is determined by the refractive index of the core and the numerical aperture (NA) of the optical fiber [23]. In case of a core made of silica, the minimum acceptance angle of internal incidence, which corresponds to the angle of total internal reflection, for an optical fiber with a NA of 0.24 is about 80° and that for a NA of 0.48 is about 71°.

#172755 - $15.00 USD Received 17 Jul 2012; revised 4 Sep 2012; accepted 4 Sep 2012; published 6 Sep 2012

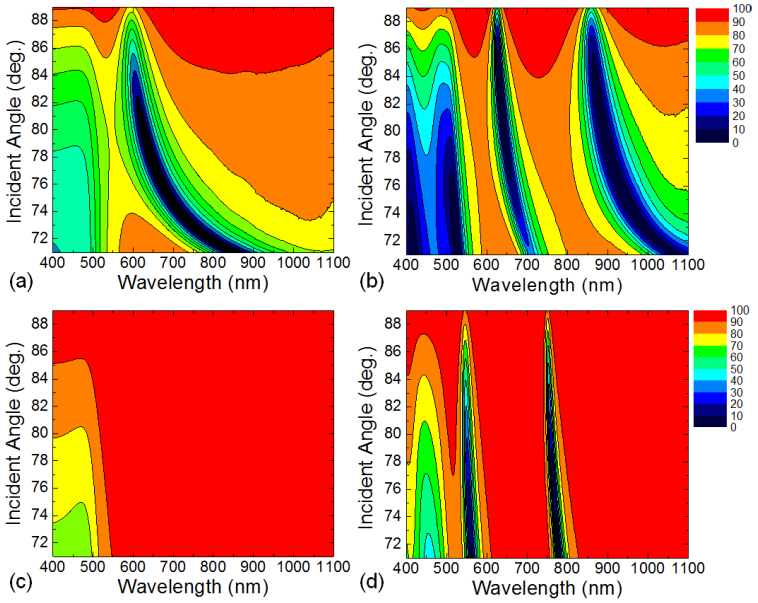

Fig. 2. Two-dimensional contour maps of internal reflectance calculated inside the silica core for both p- and s-polarization as a function of light wavelength and incident angle for the multilayer stacks of conventional Au single layer of 45 nm thickness [(a) and (c)] and waveguide coupled geometry of SiO_2 core\inner-Au layer (18 nm)\ZnS-SiO_2 waveguide (400 nm)\outer-Au layer (18 nm) [(b) and (d)] in a water buffer. The upper graphs (a) and (b) are for p-polarization, and the lower (c) and (d) for s-polarization.

Considering that the allowable NA of most of the commercially available fiber-optic based spectrometer is about 0.22 [24], the θ_i between about 80° and 90° is realistic for the silica-based fiber-optic SPR sensor. Excluding the low incident angle range of impractical high NA, the SPR wavelength is maintained around 600 nm regardless of the incident angle, as shown in Fig. 2(a). This implies that the operation wavelength is hard to be tuned even when the MMF with relatively large NA is used [11]. Such a problem of lack of tunability becomes more significant when a single-mode fiber (SMF) operating in an intensity interrogation mode is used [12, 25]. For the sensor to operate, the SPR condition should be satisfied within the refractive index range of the medium to be measured. And, to improve signal linearity and sensitivity, it is favorable that measurement be made slightly away from the resonance dip or at a highest-slope wavelength position for an optimum signal contrast. However, since the light source is the only control parameter to satisfy these requirements in the conventional sensor, a continuously tunable light source in a broad range is needed, which renders the device impractical.

The multiple reflectance dips [Fig. 2(b)] observed for p-wave in the WCSPR configuration might be ascribed to the multiple coupling to the surface plasmon mode from the optical waveguide modes. This implies that the spectral location of SPR dips can be controlled by simply changing the waveguide thickness. In addition, the narrow width may be beneficial for enhancing the resolution of sensor when operated in the wavelength interrogation mode.

The characteristics of reflectance dips shown in the Figs. 2(b) and 2(d) were examined in more detail. Figure 3 compares the spatial distribution of E-field amplitudes calculated along the WCSPR stack thickness at the dips of 640 nm for p-polarization and 757 nm for s-polarization when the incident angle is assumed to be fixed at 81°. The former shows a characteristic distribution of E-field component of p-polarized light perpendicular to the metal surface ($E_{P\_Perpendicular}$) in SPR mode, where the field maximum is located near the Au surface and decay exponentially to the environment. On the other hand, the latter represents the

#172755 - $15.00 USD Received 17 Jul 2012; revised 4 Sep 2012; accepted 4 Sep 2012; published 6 Sep 2012

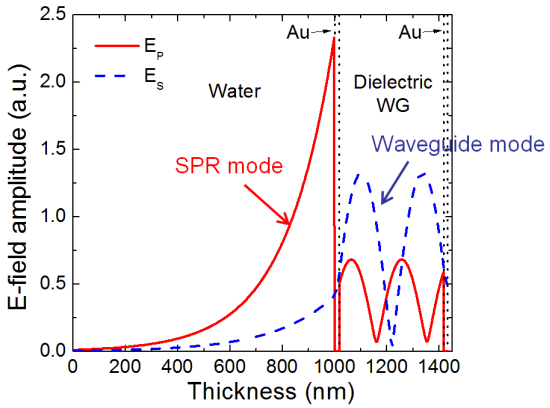

Fig. 3. Characteristic distribution of E-field amplitudes calculated along the stack thickness at the reflectance dips of 640 nm from Fig. 2(b) for p-polarization and 757 nm from Fig. 2(d) for s-polarization (waveguide mode) when the incident angle is assumed to be fixed at 81°.

characteristic field distribution of waveguide mode where the most energy is confined in the waveguide region and only a little portion of E-field leaks to the outside.

The quite different E-field distribution occurring at the interface with the external medium leads to a significant difference in sensitivity between the SPR mode and the waveguide mode. It is expected that the waveguide mode undergoes less perturbation by the surrounding index change when compared with the plasmonic mode. In other words, the plasmonic mode would sensitively response to the environmental index change but the waveguide mode wouldn't. Therefore, utilizing the waveguide mode, the change in the signal caused by the system noise factors such as the fluctuation in light source, the index change due to the temperature increase, and etc. can be corrected. That is to say, by comparing the signal from both modes, the system noise component reflected in the waveguide mode signal may be removed from the plasmonic mode signal so that the pure signal change induced by an analyte of interest can be detected. This characteristic might provide a capability of self-referencing.

Figure 4 shows 2D contour map of p-wave reflectance calculated for the WCSPR stack as a function of thickness of the ZnS-SiO_2 waveguide layer and wavelength of incident light. The incident angle was fixed at 81°. It can be seen that the number of plasmonic modes increases with the thickness of the waveguide layer. It proves that the coupling between the

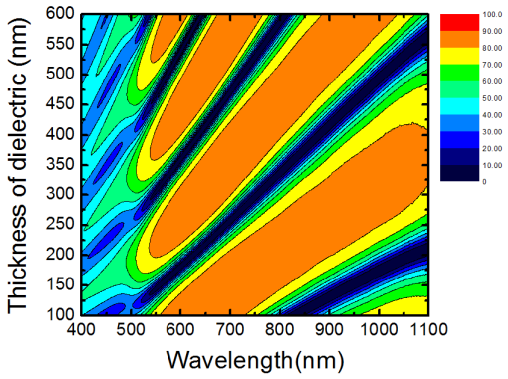

Fig. 4. Two-dimensional contour map of p-wave reflectance calculated as a function of thickness of the ZnS-SiO_2 waveguide and wavelength of incident light for the WCSPR stack having the same thickness of 18 nm for both inner and outer Au layers in a water buffer. The incident angle was fixed at 81°.

#172755 - $15.00 USD Received 17 Jul 2012; revised 4 Sep 2012; accepted 4 Sep 2012; published 6 Sep 2012

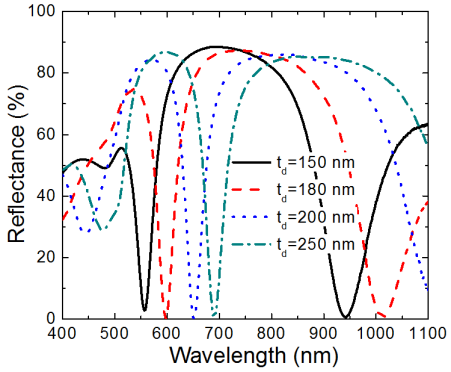

Fig. 5. Spectral reflectance line profiles taken from Fig. 4 at fixed four different thicknesses of dielectric waveguide, t_d = 150, 180, 200, and 250 nm.

plasmonic and optical waveguide modes occurs in multiple numbers with periodicity dependent on the thickness of the waveguide layer. It is understandable if we consider that there exist multiple solutions satisfying the phase matching condition between the fiber core mode to the waveguide mode in WCSPR stack even if the incident angle defined inside the fiber core was fixed. It means that the multiple guided modes have almost the same tangential wavevector and therefore can be phase matched to excite the multiple plamonic modes at the interface between the waveguide and the outer-metal layer.

Another key feature to be noted in Fig. 4 is that the spectral shift in SPR dips is continuous and linearly proportional to the thickness of dielectric waveguide. For clarity, several horizontal line profiles were taken from the Fig. 4 at different waveguide thicknesses and shown in Fig. 5. Increase in the waveguide thickness red-shifts the SPR wavelength and the extent of red-shift becomes larger in the long-wavelength mode. It is apparent that the WCSPR stack has excellent wavelength tunability only via the control of the thickness of the optical waveguide layer. This indicates that the operation wavelength can be precisely adjusted by a plasmonic stack design, which is especially beneficial when applied to single- or few-mode fibers and increases the degree of freedom for sensor optimization with a light source of any wavelength. The reflectance dips appear at the left edge below 500 nm may be ascribed to the interband absorption of the metal itself.

Figure 6 shows the calculated response of the fiber-optic WCSPR sensor to the change in the refractive index of surrounding medium when random polarized light having p- and s-polarized components mixed is incident at θ_i of 81°. The stack used in calculation was SiO_2 core\inner-Au layer (18 nm)\ZnS-SiO_2 waveguide (400 nm)\outer-Au layer (18 nm) and the refractive index of surrounding was changed from 1.332 to 1.38. The reflectance dips occurring around 640 nm and 887 nm correspond to the SPR modes generated by the p-polarized component of the incident light. And, the dips around 550 nm and 757 nm correspond to the waveguide modes by the s-polarized component.

As shown in the Fig. 6, SPR and waveguide modes are significantly different in sensitivity. The SPR modes respond very sensitively to the environmental change causing the resonance wavelength to red-shift with increasing the refractive index of surrounding medium, while the optical waveguide modes exhibit little change. Nonetheless, the waveguide modes would undergo a change arising from the system noise such as fluctuation of the light source intensity, variation in the optical constants of the materials constituting the sensor due to the temperature change of the system, and etc., like the SPR modes. Therefore, self-referenced compensation for pure SPR signal becomes possible at the identically shared sensing surface by employing the waveguide mode as a reference. A similar distinction in sensitivities between the s- and p- polarization modes can be found as a self-referencing scheme in the metal coated tilted fiber Bragg grating sensors [26].

The difference in sensitivity of the multiple modes of SPR is also noticeable in the Fig. 6.

#172755 - $15.00 USD Received 17 Jul 2012; revised 4 Sep 2012; accepted 4 Sep 2012; published 6 Sep 2012

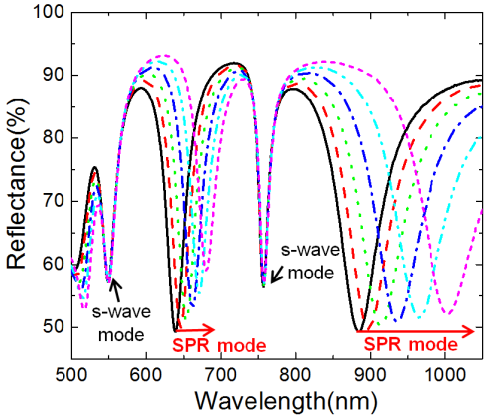

Fig. 6. Calculated response of the fiber-optic WCSPR sensor to the change in refractive index of surrounding medium when random polarized light having p- and s-wave components mixed is incident at θ_i of 81°. The stack used in this calculation is SiO_2 core\inner-Au layer (18 nm)\ZnS-SiO_2 waveguide (400 nm)\outer-Au layer (18 nm).

The sensitivity defined as the dip wavelength shift with respect to the refractive index change is 828 nm/RIU for the short-wavelength SPR mode near 640 nm and it appears to be greatly improved to the value of 2,017 nm/RIU for the long-wavelength mode at near-infrared region of 887 nm. The operation in the infrared region facilitated by our approach has additional advantages in measuring analytes relatively farther from the sensor surface or the whole cell detection, because the decay length of the local E-field becomes largely extended [27, 28]. Besides, the sensor sensitivity can be improved further through interaction with the molecular vibration mode and the spectroscopic analysis based on energy transfer may be possible in the infrared region [29].

Figure 7 shows an additional controllability by other geometrical parameters. The stack used in this calculation was SiO_2 core\inner-Au layer (18 nm)\ZnS-SiO_2 waveguide (220 nm)\outer-Au layer (touter_Au nm) in a water buffer and the incident angle was assumed to be fixed to 81°. It is very interesting that the long-wavelength mode dip goes away from the shorter one as the thickness of outer Au decreases, while the waveguide mode dips shows little shift and their depths are only changed (not shown here). These characteristics have practical importance because it can be used to adjust the sensor to avoid an overlap between the p- and s-wave mode dips when random polarized light source is used.

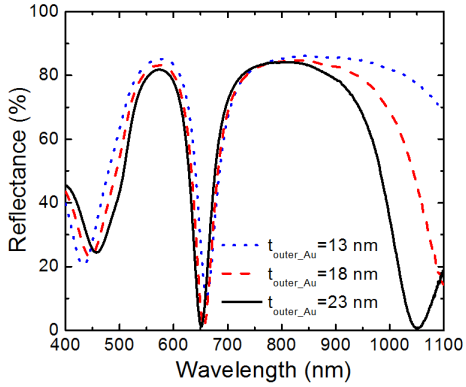

Fig. 7. Effect of thickness variation of outer-Au layer relative to that of inner-Au on the p-wave reflectance spectra calculated for the WCSPR stack of SiO_2 core\inner-Au layer (18 nm)\ZnS-SiO_2 waveguide (220 nm)\outer-Au layer (t_{outer_Au} nm) in a water buffer at a fixed incident angle of 81°.

#172755 - $15.00 USD Received 17 Jul 2012; revised 4 Sep 2012; accepted 4 Sep 2012; published 6 Sep 2012

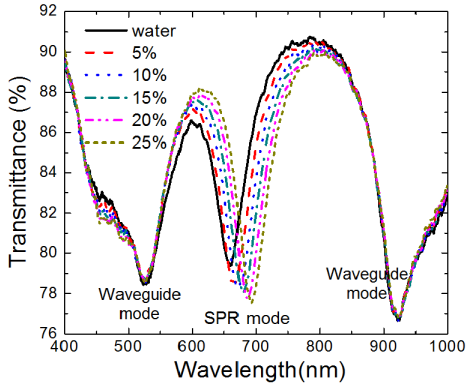

Fig. 8. Transmittance spectra measured for the fiber-optic WCSPR sensor fabricated with a stack of inner-Au (18 nm)\ZnS-SiO_2 (220 nm)\outer-Au (18 nm) while flowing the aqueous solutions of sucrose with varying the concentration from 0 to 25 w/w%.

For the experimental demonstration of feasibility, we fabricated and analyzed the fiber-optic WCSPR sensor with a stack of inner-Au (18 nm)\ZnS-SiO_2 (220 nm)\outer-Au (18 nm). Figure 8 shows the transmittance spectra measured by flowing the aqueous solutions of sucrose with varying the concentration, 0 ~25 w/w%. The measured spectra exhibits three transmittance dips; center one is from the plasmonic mode caused by p-polarized light component and the others is ascribed to the waveguide modes coupled to the dielectric waveguide by s-polarized one. It should be noted here that the guided modes seem to be immune to the change in the surrounding index while the SPR mode shifts to longer wavelength region, which is in good agreement with our theoretical prediction. The sensitivity of SPR mode was estimated to be 914.5 nm/RIU.

Figure 9 verifies the feasible self-referencing by s-wave mode for extracting the pure SPR response signal from a system noise. When we were monitoring a temporal response of transmitted intensity at the highest slope position of dip curves, a gradual decrease in the s-wave mode intensity with time and a sudden drop were observed as indicated in the Fig. 9. Those would be from the light source fluctuation. Of course, the SPR mode seems to undergo the same fluctuation. So, the system noise can be corrected by normalize the measured SPR signal by s-wave mode reference. The decreasing slope was flattened and the drop was corrected. Pure plasmonic response was then successfully obtained.

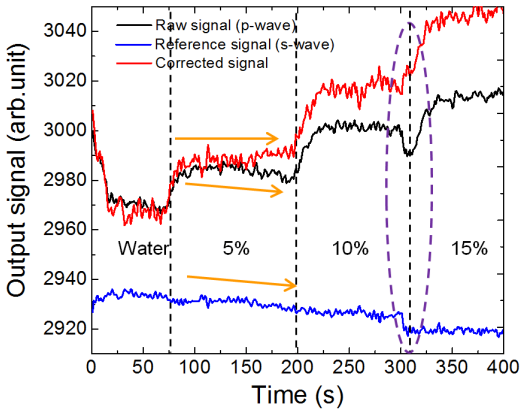

Fig. 9. Temporal responses of transmitted intensity measured at the highest slope position of dip curves from both the SPR and the waveguide modes for the experimental WCSPR stack with respect to the injection of dilute sucrose solutions, and the self-referenced SPR mode signal extracted after correction using the waveguide mode reflectance.

#172755 - $15.00 USD Received 17 Jul 2012; revised 4 Sep 2012; accepted 4 Sep 2012; published 6 Sep 2012

7. Conclusion

We suggested and demonstrated a fiber-optic WCSPR sensor. Theoretical simulation showed that the SPR wavelength can be easily controlled in a broad range from visible to infrared region via the adjustment of the thickness of dielectric waveguide inserted between two metal layers. Higher sensitivity was expected for the plasmonic modes in the region of infrared wavelength where the expanded penetration depth of local E-field and molecular selectivity can be provided. Multiple plasmonic modes are observed to be periodically generated by increasing the thickness of waveguide layer and may be selectively used for enhancing the sensor performance depending on applications. Experimental feasibility test on the sensor operation using the model WCSPR stack was successfully carried out and a potential self-referencing functionality using a waveguide mode generated in the dielectric waveguide due to the s-polarized light component was also confirmed. These characteristics would contribute for greatly enhancing the sensing performance of fiber-optic surface plasmon resonance sensors.

Acknowledgments

This research was supported by a “Center for Nanostructured Materials Technology” grant (code #: 2011K000204) under the “21st Century Frontier R&D Program” of the Ministry of Science and Technology, Korea and by an institutional program grant (2E22733) from Korea Institute of Science and Technology.

#172755 - $15.00 USD Received 17 Jul 2012; revised 4 Sep 2012; accepted 4 Sep 2012; published 6 Sep 2012